Journal of Human Evolution 59 (2010) 306–320

Contents lists available at ScienceDirect

Journal of Human Evolution

journal homepage: www.elsevier.com/locate/jhevol

Multidimensional GIS modeling of magnetic mineralogy as a proxy for fire use and spatial patterning: Evidence from the Middle Stone Age bearing sea cave of Pinnacle Point 13B (Western Cape, South Africa)☆

Andy I.R. Herries [a,*], Erich C. Fisher [b]

[a] UNSW Archaeomagnetism Laboratory, (iPAST) integrative Palaeoecological and Anthropological Studies, School of Medical Sciences, University of New South Wales, 2052, Kensington, Australia
[b] Department of Anthropology, College of Liberal Arts and Sciences, University of Florida, USA

ARTICLE INFO

Article history:
Received 22 October 2008
Accepted 29 May 2010

Keywords:
Mineral magnetism
Anthropogenic alteration
Magnetic susceptibility
mDGIS
MSA

ABSTRACT

This paper aims to identify the spatial patterning of burning and occupation within an early Middle Stone Age (MSA) sea cave in the Western Cape Province of South Africa by creating a multidimensional model of archaeomagnetic data recovered from all excavated units. Magnetic susceptibility and other mineral magnetic parameters are shown to provide an excellent proxy for the anthropogenic alteration and spread of burnt material into the surrounding unaltered cave deposits. The identification of combustion features and areas of occupation or different activities within the site can be determined because the movement of people throughout the cave mixes magnetically strong hearth material with magnetically weak unaltered sediments. This is also indicated by micromorphological analysis. The degree of enhancement is also shown to indicate the extent to which a deposit has been altered, and therefore, intensity of occupation, because multiple heatings of deposits are needed to form the concentrations of iron minerals occurring in some layers. This is further supported by a comparison with artifact density for the layers. Variation in the magnetic values between different areas of the site is noted with major occupation or fire building occurring in the front of the cave during earlier MIS 6 periods, while during later MIS 5 periods the entire cave is occupied intensively. The oldest, MIS 11 deposits at the rear of the cave indicate no evidence of enhancement and an apparent absence of any anthropogenic signature.

Introduction

The identification of spatial patterning in archaeological sites and any inherent behavioral implications remain a difficult thing to access in many Paleolithic sites. This paper aims to identify spatial patterning in an early Middle Stone Age (MSA) sea cave (Pinnacle Point Cave 13B [PP13B]) on the southern cape coast of South Africa, by creating a multidimensional model of mineral magnetic data recovered from all excavated units. Magnetic susceptibility (MS) is the most widely used mineral magnetic parameter in archaeological studies. MS is essentially the ease with which a material can be magnetized and an indicator of the bulk iron concentration within a sediment/soil/material. MS has been shown to be a powerful tool for identifying evidence for human occupation, mainly due to the use of fire at archaeological sites (Peters et al., 2000, 2002; Peters and Batt, 2002; Marwick, 2005; Church et al., 2007).

LeBorgne (1955, 1960) demonstrated that burning leads to an enhancement of the MS of soils. MS enhancement occurs because burning causes the formation of magnetically stronger, fine to ultrafine, ferrimagnetic minerals (magnetite, maghemite) that dominate the signal and mask any weaker antiferromagnetic (goethite, hematite) or larger grained ferrimagnetic phases (Morinaga et al., 1999; Peters and Thompson, 1999). While MS is often a good proxy for burning, only detailed mineral magnetic characterization will explain the complex mineralogy of natural samples and associated reason for MS enhancement or variation (see Supplementary Online Material [SOM] for a detailed review of methods). An understanding of the variation of the different mineral populations can elucidate a number of processes including sediment input, alteration, human occupation, and climate change (Herries, 2009).

In cave sites, where pedogenesis does not alter the deposits after or during deposition, MS variation is normally related to

☆ This article is part of 'The Middle Stone Age at Pinnacle Point Site 13B, a Coastal Cave near Mossel Bay (Western Cape Province, South Africa)' Special Issue.

* Corresponding author.
E-mail addresses: andyherries@yahoo.co.uk, a.herries@unsw.edu.au (A.I.R. Herries).

0047-2484/$ – see front matter © 2010 Elsevier Ltd. All rights reserved.
doi:10.1016/j.jhevol.2010.07.012

variation in sedimentary input, and in archaeological sites, anthropogenic alteration. Complex magnetic transformations can still occur in caves due to natural processes such as waterlogging and reactions related to deep guano deposits. Examples of this are the colored MSA deposits of Rainbow Cave and the Earlier Stone Age (ESA) deposits of the Cave of Hearths at Makapansgat, originally interpreted as being hearths (Mason, 1988; Latham and Herries, 2004). However, detailed magnetic mineralogical studies have identified such deposits as entirely natural and not related to burning (Herries and Latham, 2009). Variations in sedimentary input can also show evidence for climatic change in many circumstances as this changes the magnetic minerals deposited in the caves, as is the case at Rose Cottage Cave (Herries and Latham, 2003, 2009). However, when intense human occupation occurs, such as at Sibudu Cave, this natural signature is partly overprinted by anthropogenic alteration related to fire use (Herries, 2006). In such situations, layers or areas with relatively high MS values (hot spots), when compared to base sediments, should primarily represent combustion features where sediments have been altered by heat with the formation of highly magnetic mineral phases (Herries, 2009).

MS alone is generally unable to unequivocally identify *in situ* burnt material as high MS areas may represent dumped burnt material from behavior such as the raking out of hearths. However, mineral magnetic studies can be a powerful tool when integrated with micromorphology and paleomagnetic studies of burnt rocks (see Herries [2009] and Brown et al. [2009] for methodology; Fig. 1). These can identify both the maximum temperature that the rocks have experienced and whether they are *in situ* or not. Unless post burning alteration or scattering has occurred, burnt deposits should always have higher MS values than the surrounding sediments, and in many cases in South Africa *in situ* combustion features appear to have a distinct mineral magnetic signature consisting of high MS values and low frequency dependence of magnetic susceptibility (see [SOM]). Exceptions occur where deposits have been heated to high temperatures that are generally only found in kilns. (Such temperatures are rarely, if ever, generated by prehistoric campfires), or if altered by secondary natural processes such as extensive waterlogging (Herries and Latham, 2009).

Diffusion of burnt material throughout archaeological deposits by occupation causes dilution of the magnetic hot spots and enhances the surrounding weakly magnetic, unburnt material with the addition of highly magnetic altered material. In theory, the MS data combined with other methods have the ability to identify *in situ* combustion features and the area of occupation used by humans around these features (or over time in vertical layers). This is because human movement spreads combusted material into the surrounding weaker deposits as humans move around the cave after having built a fire. However, other mechanisms (fluvial, aeolian) can also be responsible for diffusion of burnt material, and therefore other analyses such as micromorphology are useful for understanding general processes occurring in the deposit (see Karkanas and Goldberg, 2010). A comprehensive survey of the MS of sediments excavated from an archaeological site can expand the interpretive range of other bulk point sampling methods (micromorphology, Fourier transform infrared spectroscopy [FTIR]) to easily include every excavated lens and feature at the site. Such microsampling is possible because MS measurements have the advantage of being cheap and easy to undertake and sample sizes are small, on the order of 10 g of sediment.

One of the main limitations in interpreting MS data has been visualization, which has mostly relied upon two-dimensional sections or occasionally areal surveys (Ellwood et al., 1997; Herries and Latham, 2003; Herries, 2006, 2009). To visualize the MS of every single excavated unit from an archaeological site, as attempted in this study, multidimensional visualization is necessary. Multidimensional visualization and analysis are more popular than ever now because of cheaper, more powerful software and newer techniques and equipment to record data precisely in 3D. As digital data are increased, multidimensional visualization is becoming a naturally useful tool to efficiently and intuitively interact with and

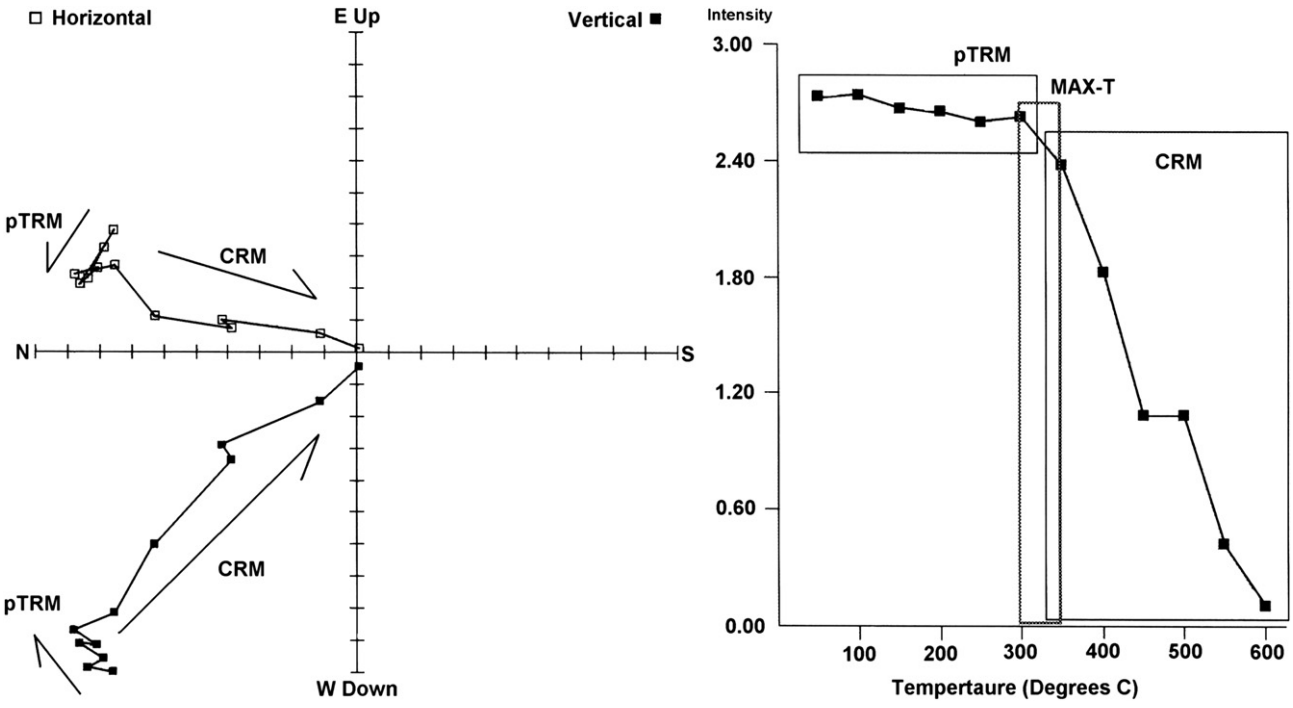

Fig. 1. Paleomagnetic analysis (zijderveld and intensity plots [A/m^2]) of sample 46660 from the LC-MSA (Northeastern area excavation). The pTRM from the heating is removed by between 300 and 350 °C to reveal the primary geological remanence (CRM).

comprehend complex data sets. Within an archaeological setting, this intimacy with the spatial data allows unprecedented access into the often complex spatiotemporal patterns of archaeological materials and their relationship to other natural or cultural features.

However, while archaeological data are now more often being recorded in 3D, for example using total stations, the GIS-based spatial analysis of these data still seems to be predominantly within a 2D framework. The reason for this is likely due to specific deficiencies of 2.5D–4D visualization and spatial analysis within current readily available, and affordable, software utilizing a true GIS framework, which are also not dependent upon advanced computer programming or graphics training (Zlatanova et al., 2004). Much progress has also been made on the visualization of archaeological sites and data using virtual reality techniques including photogrammetry (e.g., Pollefeys et al., 2003; Barceló and Vincente, 2004) and digital 3D scanners (e.g., Redfern and Kilfeather, 2004) to create shape models of archaeological structures or objects (see also Barceló [2000]). While these applications are certainly useful, the accuracy of the models and, more specifically, their ability to be tested and refined against a series of working hypotheses can be questioned based on the perceived preferences for visual aesthetics by the various authors[1] (for similar, see Lewin and Gross [1997]; Boukhari [2000]).

This study relies on the recent Multidimensional Geographic Information Systems (mDGIS) approach which, at its core, seeks to conjoin accurate and aesthetically pleasing visual effects with quantitative hypothesis driven and testable spatial models. mDGIS is defined as the representation and analysis of spatial and non-spatial data within a dynamic visual environment that facilitates 2.5D non-volumetric depth of field, 3D volumetric representation, and 4D time and movement (see also Fisher [2005, 2007]). In this study, the mDGIS approach allows us not only to view the complex spatial relationships among data but develop testable spatial models on the distributions and densities of MS, archaeological, and geological data to understand better how the sites were occupied within and across different times.

Overall this study had a number of specific aims: (1) create the first multidimensional model of mineral magnetic data from a Paleolithic site, (2) identify if high MS values correlate with features identified as burnt during excavation, (3) compare interpretations from MS and micromorphology data (Karkanas and Goldberg, 2010) regarding *in situ* combustion features, and (4) identify if MS data indicate differences between units in each excavation area, and if there is a difference between excavation areas that might indicate changes in the spread of anthropogenically altered material and, therefore, occupation (or activity specific areas within the site) of the site through time.

Site Chronology

The chronology of the PP13B sediments is developed from optically stimulated luminescence dating (OSL) and U–Th dating. The OSL results are described in Jacobs (2010), while the U–Th results and stratigraphy are described in detail in Marean et al. (2007, 2010). All age estimates used in this paper come from these papers, and the following summary is developed from those data (see also Table 1). A conservative age spread is provided by taking the minimum and maximum OSL ages from each stratigraphic unit, adding 1 sigma to each, and then adjusting these for U–Th ages that are intercalated. For example, the more precise U–Th ages on clean speleothems directly contacting the top of the archaeological sediments shows us that the cave closed no later than 91 ka, so that age is used to adjust the age span of underlying OSL-dated sediments to no younger than 91 ka.

Excavations were undertaken in three areas of the cave: the Northeastern area or LC-MSA, the Eastern area at the front of the cave, and the Western area at the rear of the cave (Fig. 6). The oldest deposits are a series of archaeologically sterile Laminated Silts that are preserved in the Western area at the rear of the cave and date to MIS 11 (414–349 ka). The Laminated silts were then eroded before deposition of sediments dated to MIS 6, from roughly 174 to 142 ka. These MIS 6 deposits are preserved at the rear of the cave as uncalcified sandy deposits (DB Sand 4 deposits) and in the front of the cave as a series of heavily eroded calcified deposits on the wall of the cave (LC-MSA Lower). The next phase of deposition occurred between roughly 133 and 115 ka at the beginning of MIS 5 and again consists of calcified deposits at the front of the cave (LC-MSA Upper lower dune and LC-MSA Middle), and perhaps a series of loose deposits at the rear of the cave (LBG Sand 1). A significant phase of erosion then appears to have occurred before the deposition of the Lower Roof Spall in the entrance area (Eastern area) of the cave between 114 and 106 ka. This initial deposition was then followed by the deposition of a series of uncalcified deposits in both the front and the rear of the cave between 102 and 91 ka (see Table 1). At 91 ka the cave was sealed by a large dune and speleothems began to form on the back slope of the dune surface.

Methods

Archaeomagnetic sampling and laboratory analysis

Bulk samples were taken from every stratigraphic unit (StratUnit) that was identified from the three excavations at the site and are presented as project sample numbers unless otherwise stated (see Marean et al. [2010]). Subsamples of the bulk sample were then sieved to remove large clasts of quartzite, air dried for 48 h, and packaged into standard paleomagnetic sample cubes before shipment to the laboratory in Liverpool. This process saves shipping more sediment than is necessary and so reduces the overall costs of analysis. StratUnits are grouped together to form stratigraphic aggregates (StratAggs), representing a distinct phase of deposition. The data we further contrasted against micromorphologically distinct units as per Karkanas and Goldberg (2010). When large StratUnits were encountered multiple samples were taken from different excavation squares to increase sample density. Samples were taken from bulk samples so as to represent the average of the deposit sampled. The samples were packaged into standard paleomagnetic sample cubes. In total, around 676 bulk samples were studied from the three excavation areas (Northeastern [LC-MSA], Western, and Eastern), which did not include surface cleanings and disturbances.

Standard dual frequency magnetic susceptibility methods were applied as per Dearing (1999) and are presented as low frequency magnetic susceptibility (MS or χ_{LF}) measurements in units of $10^{-8}\,m^3\,kg^{-1}$ unless otherwise stated. A series of more detailed mineral magnetic tests (as per Walden et al. [1999]) were conducted on representative samples to identify the magnetic mineralogy, grain size, and concentration of magnetic minerals giving rise to the MS variation (see SOM). The magnetic susceptibility of the samples at dual frequency room temperature (X_{LF}, X_{HF}, X_{FD}%) and from liquid nitrogen temperatures (−196 °C; MS-LT) were conducted on Bartington (Ltd.) MS2 equipment. A Magnetic Measurements (Ltd.) Variable Field Translation Balance (VFTB) was used to perform isothermal remanent magnetization (IRM)

[1] It should be noted that not all archaeologically based virtual reality (VR) applications are inaccurate, but rather that they are missing a spatial analytical component.

Table 1
Mean, minimum, and maximum magnetic susceptibility (MS) values, age estimates, and location of major stratigraphic aggregates from PP Cave 13B

Strat aggregate	Magnetic susceptibility (10^{-8} m^3 kg^{-1})					Age min (ka)	Age max (ka)	Age median (ka)	Excavation
	No.	Mean	Min	Max	s.d.				
LB Sand 1	38	10.45	1.38	32.47	5.79	91	94	93	Western
Shelly Brown Sand	25	35.93	22.22	55.17	8.87	91	98	95	Eastern
Upper Roof Spall	86	52.45	17.61	414.01	43.55	91	98	95	Eastern
DB Sand 2	11	18.16	10.38	29.92	7.08	91	102	97	Western
LB Sand 2	6	13.44	2.55	22.87	6.81	91	102	97	Western
DB Sand 3	79	30.01	2.42	150	32.93	91	102	97	Western
Lower Roof Spall	37	40.97	5.76	138.99	34.8	106	114	110	Eastern
LBG Sand 1	93	4.74	0.2	26.32	3.62	94	134	114	Western
LC-MSA Upper	9	25.66	7.91	61.3	17.87	115	133	124	Northeastern
LC-MSA Middle	25	43.84	14.85	81.01	18.03	120	130	125	Northeastern
DB Sand 4a	8	2.18	0.21	4.28	1.32	117	166	142	Western
LBG Sand 2	9	4.15	1.83	17.73	5.15	117	166	142	Western
DB Sand 4b	7	4.45	0.71	17.54	5.86	152	166	159	Western
LBG Sand 3	4	2.5	1.19	3.32	0.91	152	349	160	Western
DB Sand 4c	21	2.25	0.76	4.61	1.1	152	349	160	Western
LBG Sand 4	1	3.82	3.82	3.82	0	152	349	160	Western
LC-MSA Lower	99	56.76	4.5	153.49	28.22	153	174	164	Northeastern
LB Silt-G	11	2.03	0.65	4.32	0.97	152	349	251	Western
LB Silt	21	1.85	0.47	3.17	0.74	152	349	251	Western
Laminated Facies	12	1.27	0.72	3.33	0.71	349	414	382	Western

acquisition and backfield curves, hysteresis loops, and thermomagnetic (Curie) curves.

The mineral magnetic study at PP13B has been augmented by: (1) paleomagnetic analysis of burnt rocks to define *in situ* and *ex situ* burnt rocks (Fig. 1), and (2) micromorphological analysis of the deposits to help discriminate between deposits diffused by aeolian or anthropogenic action (see Karkanas and Goldberg [2010]).

Multidimensional GIS modeling

Multidimensional Geographic Information Systems (mDGIS) was used to contextualize MS samples within site PP13B and the corresponding geological and archaeological deposits. The study relied on ESRI ArcGIS 9.2, including the 3D Analyst extension and ESRI ArcScene, to model site PP13B. Despite noted multidimensional visualization and analytical deficiencies[2], ESRI ArcGIS is among the most widely used GIS programs available today making the data generated easily transferable and usable by other users or applications. ArcGIS also provides a comprehensive suite of tools for creating raster and vector data types and, with customization, can be manipulated sufficiently to create suitable multidimensional data. For advanced multidimensional modeling (e.g., 3D convex hulls and TIN models) Raindrop Geomagic was used.

Data within the mDGIS were mapped using Topcon reflectorless total stations georeferenced to a local, site centric grid (MAP grid). All finds, including archaeological and geological specimens, removed from the site were shot in directly with a total station. Bulk samples for the MS analysis were shot in similarly. Both plotted finds and bulk samples received unique identification numbers that were used later to associate the data with StratUnits or other attributes. StratUnits were mapped by plotting the outline and center of the upper and lower extent of each unit. In total, 34,121 plotted finds, 1070 StratUnits, and 676 MS samples have been mapped since 2000, providing a detailed archaeological and geological record of the site.

The base data of the mDGIS consists of a high-resolution 2.5D TIN model of PP13B created using Raindrop Geomagic. StratUnits containing evidence of burning as identified in the field (Field Identified Combustion Features [FICF]), such as charcoal, burnt bone or stone, and ash, were modeled as z-aware polygons. Plotted finds were similarly subdivided according to association with burnt StratUnits and represented as color coded individual points. The plotted finds associated with burnt StratUnits are thus defined as Burnt StratUnit Plotted Finds (BSUPF). While BSUPFs should occur consistently with burned StratUnits, the opposite is not always true. Thus, observation of BSUPF density within and around burned StratUnits, and also MS "hot spots," may help define activity areas, including *in situ* combustion features and secondary displacement of burned materials. MS points were modeled using size graduated 3D spheres subdivided into 12 classes corresponding to MS value ranges. MS hot spots were defined as having a MS value greater than or equal to 50.00.

Magnetic susceptibility modeling; results and discussion

The Pinnacle Point caves provide perfect testing grounds for mineral magnetic studies for a number of reasons. Firstly, the deposits are not altered by pedogenesis after deposition. While iron is mobile and susceptible to two way transformation, the magnetic mineralogy of burnt sediments is relatively stable up to ~600 °C (Herries et al., 2007) and preliminary paleomagnetic studies of burnt rocks from PP13B suggest they were heated to maximum temperatures around 300–350 °C (Herries, 2009; Fig. 1). Because PP13B is a relatively narrow deep cave that is perched part way up a sea cliff, natural fires occurring within the cave are extremely unlikely.

Secondly, the bulk of the unaltered base sediments (before archaeological occupation) consist of diamagnetic (negatively magnetic) to very weakly magnetic, externally derived 'dune sand' and internally derived 'cave sand' from breakdown of the host quartzite (SOM Fig. 1; Table Mountain Sandstone [TMS]; Karkanas and Goldberg, 2010). Mineral magnetic analysis of local dune and cave sand indicates that the cave sand was entirely devoid of ferrimagnetic material suggestive of aeolian-derived soil, while the

[2] Visualization deficiencies with ArcGIS 9.2 include: 1) limited TIN and raster surface interpolation techniques to model highly irregular and spatially restricted surfaces, 2) the inability to model topography with overhanging or vertical surfaces, 3) lack of volumetric and solid modeling techniques, and 4) the inability to create vector data (e.g., point, polyline, polygon, and z-aware shapefiles) within the 3D environment. Analytical deficiencies include: 1) the inability to perform mathematical calculations and spatial analyst functions on raster data within a 3D environment (i.e., ArcScene), and 2) limited 3D point pattern spatial analysis including 3D volumetric density analysis.

dune sand had an extremely weak signal suggesting an extremely small amount of such material (see SOM).

Thirdly, experimental fires and laboratory heating experiments produced on local Pinnacle Point dune and cave sand indicate that heating causes magnetic enhancement with an increase in MS values (Fig. 2 and SOM Fig. 1). The contrast between the unburnt and burnt deposits is very marked and so mixing of burnt material into unburnt sands is even more noticeable. Experimental fires indicate that as more fires are burnt on the same spot greater MS enhancement is seen after each successive burn and so the amount of MS enhancement could indicate the intensity of occupation (Fig. 2a). An increase in the frequency dependence of magnetic susceptibility (X_{FD}%) is also noted and indicates the formation of fine-grained ferrimagnetic minerals that have been shown to be produced by burning (Herries et al., 2007; Herries, 2009; see SOM). While some darkening of the deposits below the experimental fire occurred there was almost no enhancement of the deposits below 2 cm and very little below 1 cm (Fig. 2c). Therefore, while burning can alter the color of underlying deposits it does not secondarily alter the magnetic signal of the deposits, even after several fires. Extremely high MS values were not recorded in the experimental fires until four fires had been burnt on the same spot. After four fires the high MS values also correlated with a decrease in X_{FD}% values due to the formation of ultrafine superparamagnetic (SP) grains (see SOM for more information; SOM Fig. 3). The presence of SP grains is also confirmed by low temperature magnetic susceptibility analysis (see SOM Fig. 4). The pattern of high MS and medium to low X_{FD}% values is characteristic of *in situ* hearths from South African MSA sites (Herries, 2006, 2009; SOM). This pattern suggests that extremely high MS values may represent areas where multiple fires have been lit and where long term occupation occurred. Minimal enhancement may indicate shorter periods of occupation.

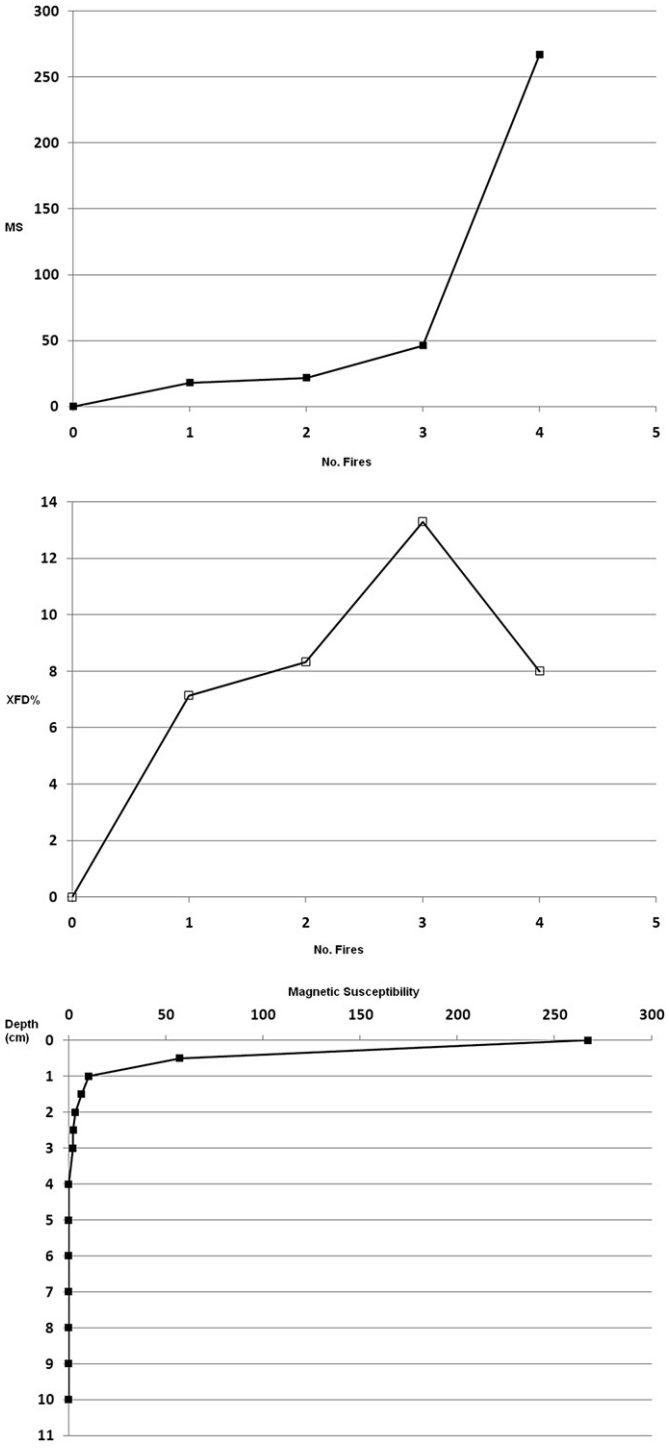

Fig. 2. Magnetic susceptibility data for experimental fires produced on Pinnacle Point cave sand. (a) Increase in magnetic susceptibility (MS) after successive burns; (b) increase and then decline in frequency dependence of magnetic susceptibility after successive burns; (c) decrease in MS with depth after the fourth successive fire.

Fourthly, the site chronology (see Marean et al. [2010]; Jacobs [2010]) suggests that sediments of a similar age occur in different parts of the cave and so changes in occupation patterns could be noted in space and time. The MS measurements for the site varied between 0.2 and 414 (10^{-8} m^3 kg^{-1}). To present the MS data in a clear format they are plotted using 2D plan and profile graphs, 3D oblique angle images, and a Supplementary video (SOM Video) discussing and visualizing the data within the mDGIS. Figure 3 shows the traditional 2D method where only single slices of MS data are shown in section. Figure 4 plots the same data within the 3D GIS model and with geospatial coordinates associated with the MS data. The SOM Video shows the model in its true multidimensional form. The model visualizes the data as spheres and the larger spheres indicate larger MS values.

Is there variation in the MS pattern between different areas?

Figures 5 and 6 show two different horizontal 2D representations of MS values for the three excavation areas. Figure 5 shows the pattern using size-graded spheres to represent MS values and

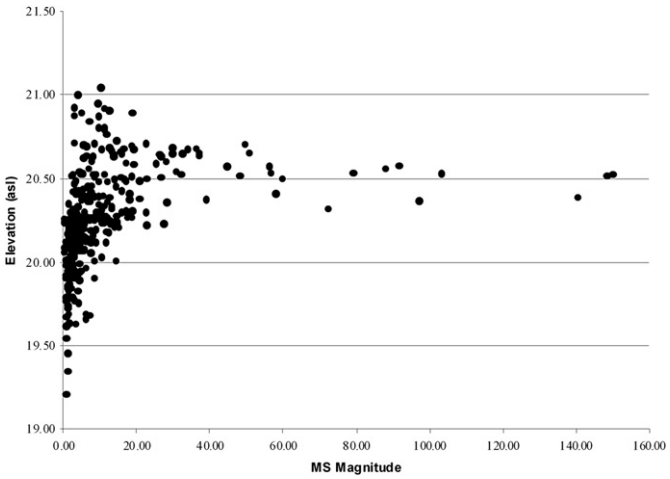

Fig. 3. MS (10^{-8} m^3 kg^{-1}) versus elevation for the Western excavation of PP13B.

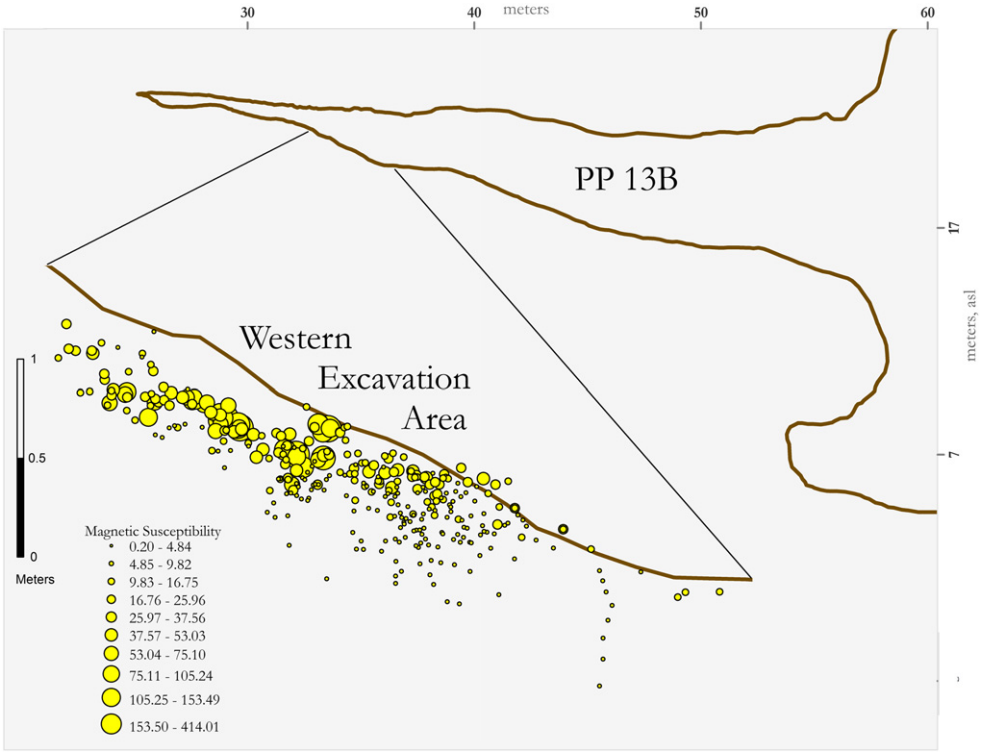

Fig. 4. A vertical slice through the PP13B GIS model for the Western area excavation. This slice shows the slope of the deposits at the rear of the cave along with the identified slope of high MS values associated with StratAgg DB Sand 3. There is an absence of high MS values in the lowest layers of this excavation. The vertical line of circles on the right of the picture represents the archaeologically sterile MIS 11 deposits. A Jenks routine was used for this and all subsequent figures.

shows the exact 3D coordinates of each sample point. In such a representation, the value of unsampled areas between sample points is not estimated. Figure 6 is a Kernel density raster calculation of the magnetic susceptibility that is often used in 2D visualization of archaeological data. However, it cannot be used in a multidimensional model and additionally it calculates values for unsampled space between sample points. It is therefore not a true reflection of the MS variability.

What is immediately apparent from both figures (Figs. 5 and 6) and Table 1 is that MS values are much higher in the front (Eastern and Northeastern [LC-MSA] excavations) of the cave when compared to the rear (Western excavation). Moreover, high MS values also cluster in definable layers. Such patterning in the data may indicate variations in anthropogenic alteration and so spatial patterning of occupation throughout the cave and through time. As shown in Figure 6, MS values are greatest from the LC-MSA deposits (mean 52.23), followed closely by the Eastern excavations (43.61), and then the Western excavations (11.34). Figure 7 and SOM Table 2 indicate that there are significant differences between the various StratAggs in each area, particularly for the Western excavations. As can be seen from Table 1 and SOM Table 2 the mean MS of the three areas is significantly different from each other and within those areas the mean MS of each of the stratigraphic aggregates is also significantly different. One of the aims of this paper was to try to understand the MS patterning both in vertical (time) and horizontal (spatial) space. As the Western area deposits show the greatest MS variation and have the longest stratigraphy, they are the main focus of this study.

What do MS hot spots represent?

A number of MS hot spots (MS > 50) are noted in the MS data from all three areas of the cave (Figs. 4–6 and 8–10). The magnetic mineralogy of hot spots from the site indicates that they are dominated by ultrafine-grained ferrimagnetic minerals consistent with that from modern fishermen's hearths in the Pinnacle Point caves (see SOM) and experimental fires (see above; Fig. 1). Frequency dependence of magnetic susceptibility (X_{FD}%) measurements of the Western area excavation MS hot spots indicate a signature that is characteristic of *in situ* combustion features with high MS and low X_{FD}% (see Fig. 1 and SOM Fig. 3).

PP13B also contains large quantities of iron oxide-rich ochre that occurs in the cave because of its use as a pigment (Marean et al., 2007). As such, the mineralogy of excavated and modern ochre was studied to assess its possible influence on the MS signal (SOM; Herries, 2009). In general, the ochre from the site has a low MS and is mainly dominated by antiferromagnetic hematite and, as such, has a distinct mineralogy compared to the burnt sediments and would very minimally influence the MS of the samples (SOM Fig. 2a). However, analysis of ochre from the Eastern area excavations indicates that some ochre has a minimal to strong ferrimagnetic signal that is similar to experimentally heated ochre (see Herries [2009]). Ferrimagnetic ochre is often deep red in color and the fact that the early modern humans at PP13B were picking the reddest ochre for utilization (Marean et al., 2007; see Watts [2010]) may indicate that they were deliberately altering the color of the ochre by heat as early as 114–91 ka or even as early as 174–153 ka.

While ochre does occur in very high density in high MS layer DB Sand 3 of the Western excavations (Fig. 8), its influence on the MS signal is minimal. Overall, ochre does not correlate with MS hot spots (Fig. 8), and in the Western area of the cave in particular the ochre is dominated by a weak antiferromagnetic mineralogy that could not be responsible for the MS hot spots, despite some association. The majority of the ferrimagnetic ochre comes from the Eastern area excavations, where the MS signal is more homogenous and perhaps suggests mixing of a number of combustion features throughout the deposit. While the ochre

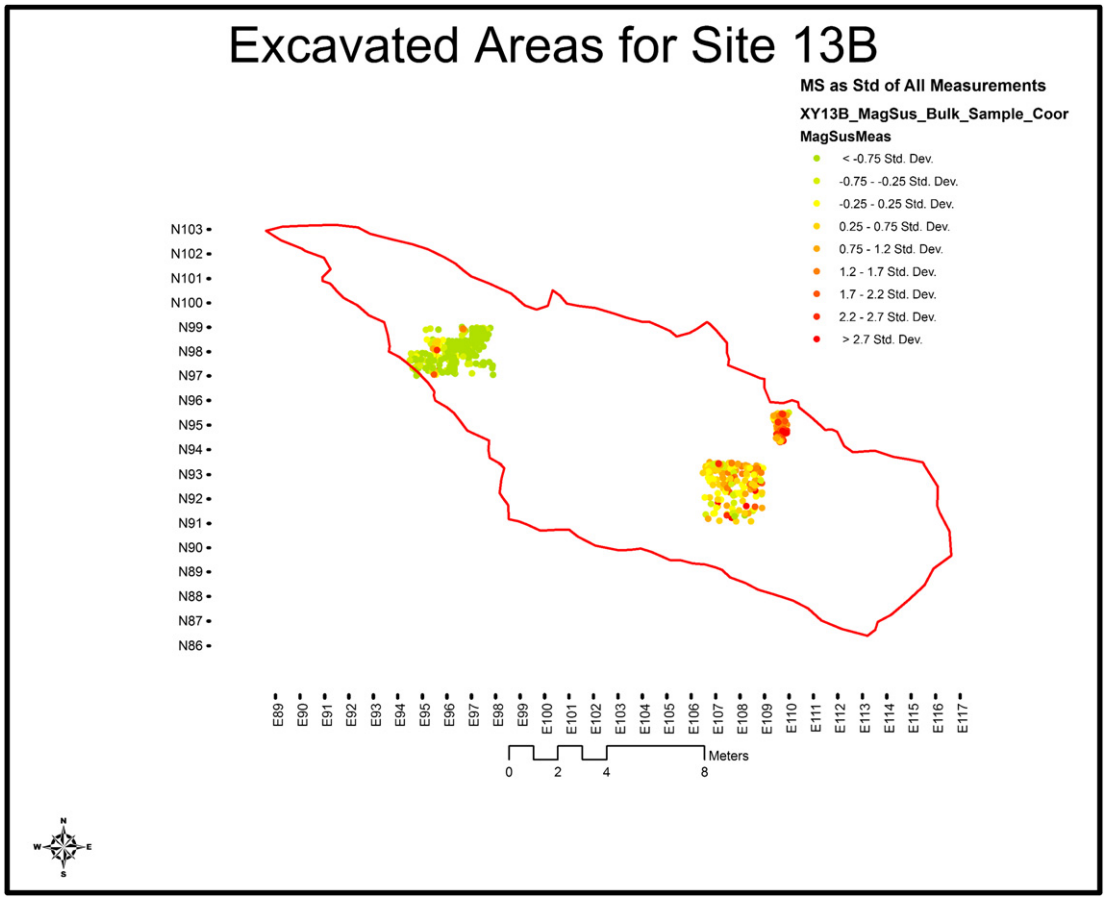

Fig. 5. Plan of Pinnacle Point Cave 13B showing the three excavation areas (Western, Eastern, and Northeastern) and their MS values. The front of the cave is to the east. MS values from the excavations at the front of the cave are noticeably higher than in the rear of the cave.

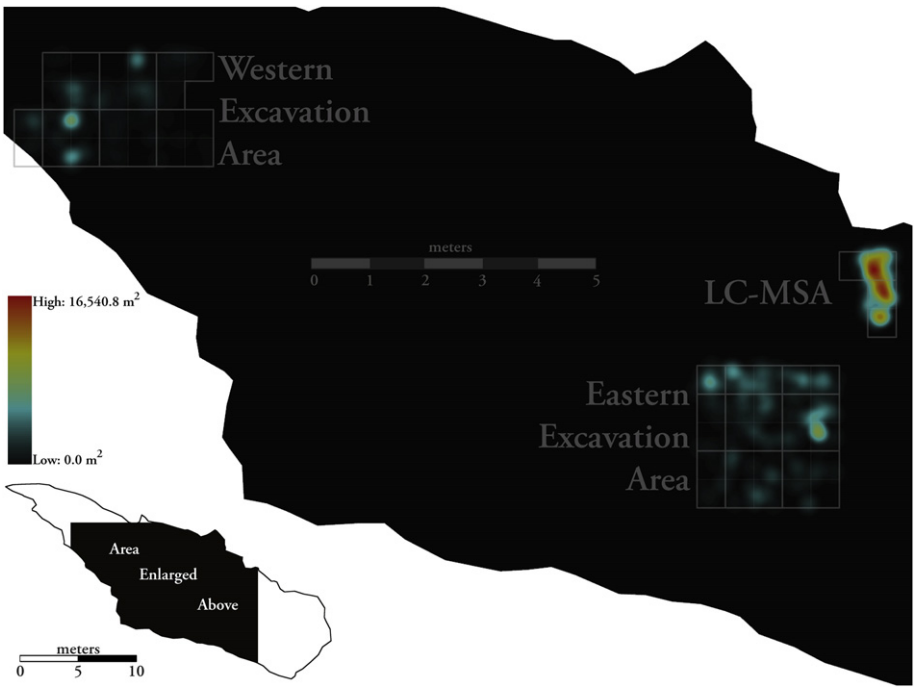

Fig. 6. Kernel density raster calculation of the MS sample values at PP13B. The density search radius was set to 0.25 m and area units refer to square meters. The resolution of the density calculation is 0.01 m.

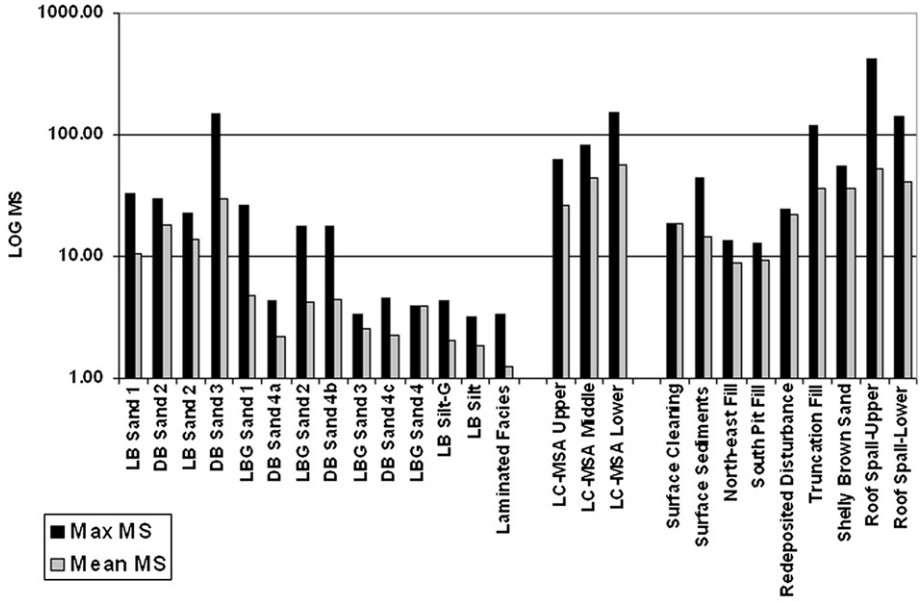

Fig. 7. Mean magnetic susceptibility (MS; 10^{-8} m^3 kg^{-1}) for the stratigraphic aggregates (StratAggs) from PP13B Western area excavation (DB Sand 2 to Laminated Facies), LC-MSA (Upper, Middle, Lower) and Eastern area excavations (Northeast to Roof Spall). The StratAggs are shown in stratigraphic order from top to bottom.

might influence the base MS signal in the cave, its effect can be detected by recovery during excavation and by more detailed mineralogical analysis. Based on this, there is little evidence to suggest that it has a major influence on the distribution of MS hot spots anywhere in the cave.

The magnetic mineralogical analysis (see SOM) supports the null hypothesis that high MS is a proxy for anthropogenic alteration due to fire use. However, MS hot spots could represent either *in situ* combustion features or dumps of combusted material. The first task was to identify if MS hot spots correlate with field identified combustion feature (FICF). Comparison of MS and MS hot spots using the mDGIS model shows that 'magnetic susceptibility identified combustion features' (MSICF) do correlate with field identified combustion feature (FICF), particularly in DB Sand 3 of the

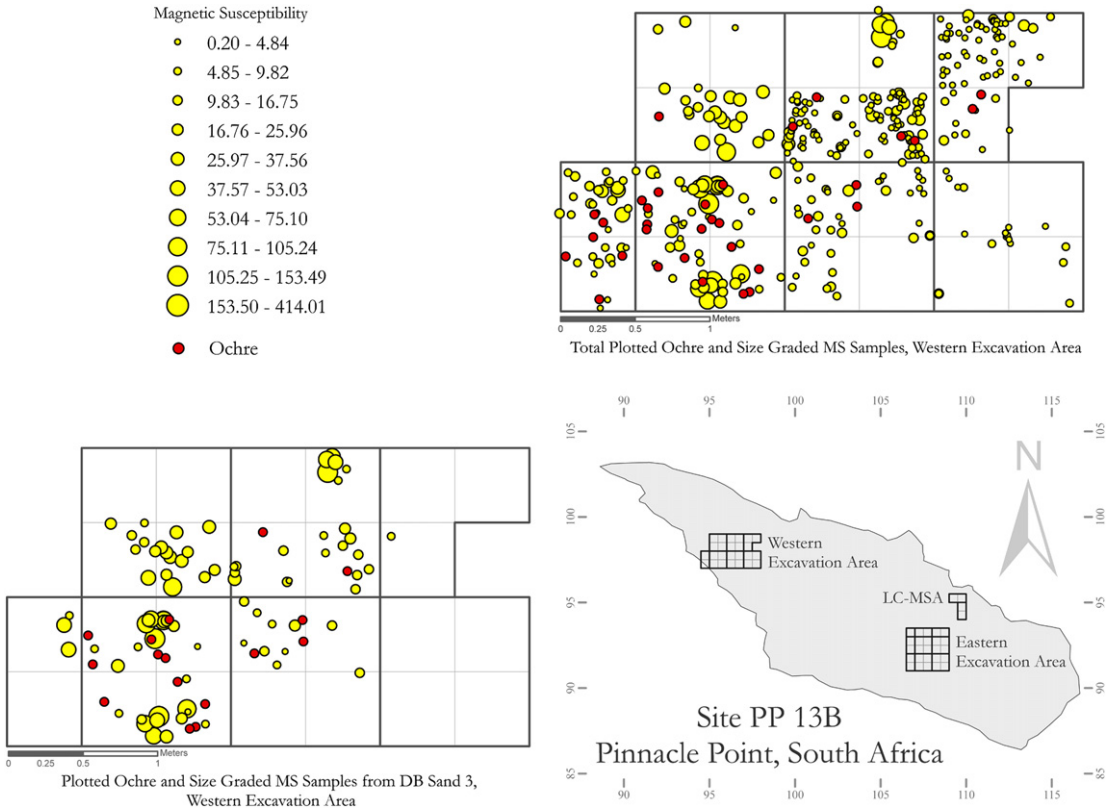

Fig. 8. The location of the three excavation areas in PP13B, as well as two-dimensional slices through the PP13B GIS model for the Western excavations showing the relationship between MS values and ochre.

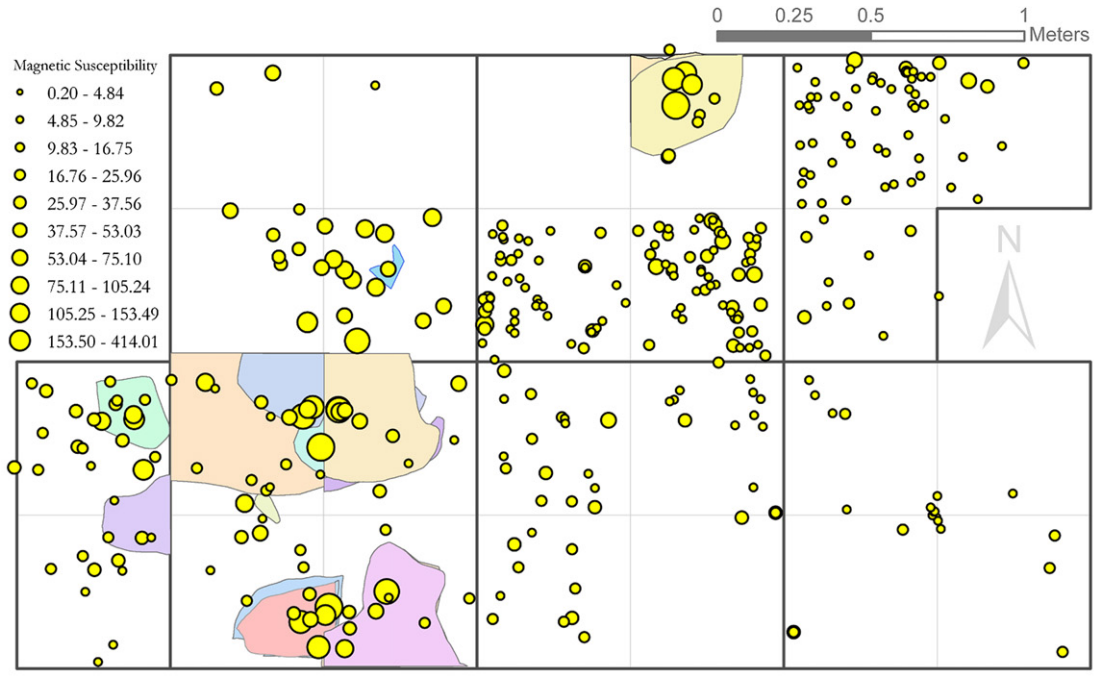

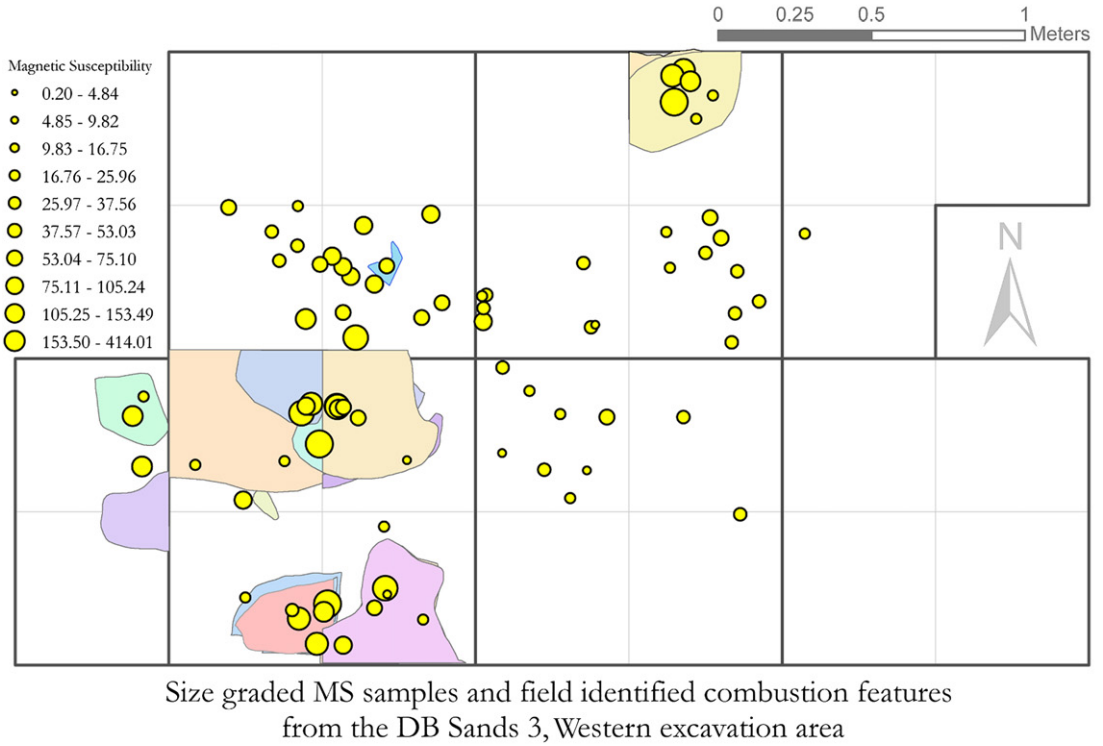

Fig. 9. A comparison between MS (10^{-8} m^3 kg^{-1}) values and field identified combustion features (FICF) from the Western excavations. The top example gives all of the data from the Western area excavations, while the lower example gives only data from the high MS StratAgg DB Sand 3. There is a clear association between MS hot spots and FICF.

Western excavation (Fig. 8; see SOM). The mean MS value of unburnt StratUnits was 25, while the mean MS value of FICF is 48. This is almost a two-fold difference and the variation is statistically significant (SOM Table 3). This is further emphasized by the fact that not all burnt units were identified correctly during excavation. Another notable feature of this analysis is the way that FICF often stop at excavation square boundaries (Fig. 9). This indicates that the identification and spatial patterning of combustion features by excavation alone can be heavily biased and subjective.

In the Western excavation 85.71% of MSICF ($n = 14$) occur within FICF, while elsewhere MS values are consistently lower (mean MS 8.14). The distribution of plotted finds from burned StratUnits (BSUPFs; $n = 2{,}090$) and MS sample intensities ($n = 195$) in the Eastern excavation also correlate well with stratigraphic

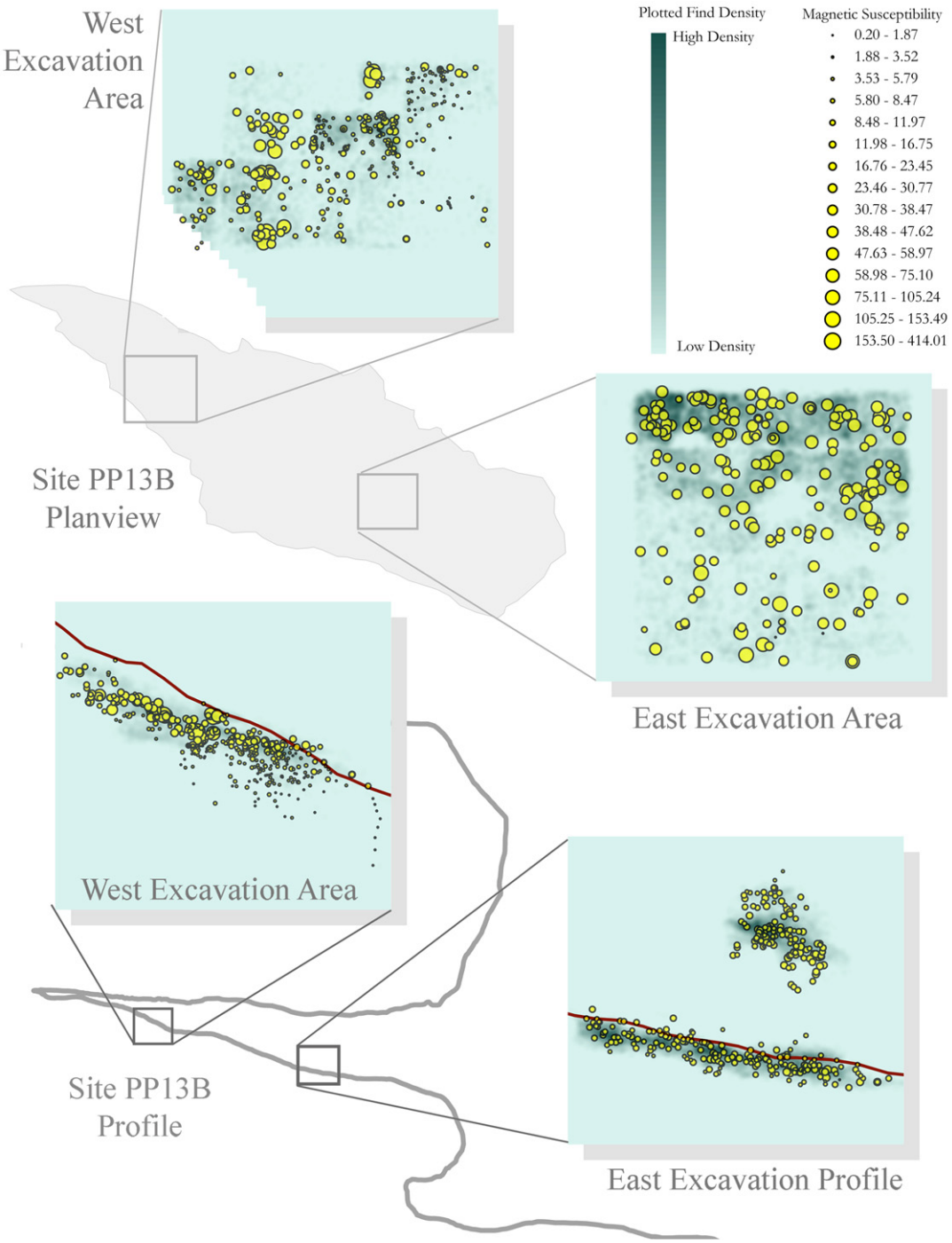

Fig. 10. MS (10^{-8} m^3 kg^{-1}) values compared against occupation density for the Eastern and Western excavations. A vertical slice is also shown through the LC-MSA deposits.

interpretations and are sloped at ~8° SSE. The vast majority (91.47%) of MS hot spots (MS > 50) here occur within the spatial extent of FICF. This correlation further supports the interpretation that MS primarily reflects burning and anthropogenic activity.

The MS data was also correlated against the micromorphological data of Karkanas and Goldberg (2010). Micromorphological analysis of deposits from the Western excavation suggests that some layers contain significant inputs of charcoal and burnt bone, which were crushed and broken as a result of trampling (for example sample 46564; Karkanas and Goldberg, 2010). This further suggests humans as the mechanism for redistribution of burnt material away from combustion features. Unfortunately, there is no micromorphology sample directly related to an MSICF in the Western area excavation. The micromorphology samples fall into areas where the MS signal is of a medium value. The MS and micromorphology together suggest that burnt material was intermixed with unaltered sand deposits due to trampling in the more Eastern part of the Western area excavation. The MS pattern suggests redistribution of burnt material down slope towards the entrance (east) of the cave, and so mixing likely occurred due to both human movement and gravity driven slope processes (Figs. 4 and 9).

In the Western area excavation, where archaeological deposits overlay archaeologically sterile sediments, a decrease in MS is seen

with depth (Figs. 3 and 4). This indicates how increased MS values are associated with archaeological horizons due to anthropogenic alteration. The distribution is not purely the result of the sloping topography as visual analysis clearly shows larger MS spheres higher in the sequence with a gradual decrease in MS sphere size with lowering elevation. Additionally, pigment and plotted find density (note: this includes archaeological and potentially also non-archaeological material) is highest within the upper stratigraphic aggregates (Figs. 8, 10, and 11). Figure 10 clearly shows a horizontal patterning in the MS values for the Western excavation with at least six MS hot spots, mostly towards the rear of the excavation area.

Western area excavation MS pattern

The Laminated Facies are the oldest deposits in the cave. They are archaeologically sterile and probably formed during MIS 11 (Jacobs, 2010). The Laminated Facies have the lowest MS values for the site (Table 1; MS 0.72–3.33), with a mean of 1.27, and have a weak antiferromagnetic mineralogy (SOM Fig. 2b). The low background MS values for these basal sediments (Figs. 4 and 7) in the Western excavation are due to breakdown of the TMS host rock and a lack of anthropogenic activity (Karkanas and Goldberg, 2010). The TMS is diamagnetic (negatively magnetic), while the resultant eroded sands range between diamagnetic and weakly antiferromagnetic. This is due to oxidization/reduction cycles during wetting and drying phases.

After a depositional hiatus in the Eastern excavation stratigraphic aggregates LB Silt, LBG Sand 3, LBG Sand 4, and DB Sand 4c continue to be dominated by internally derived silty sand. The majority of this material also has a very low MS (<5) and has remained essentially unaltered, despite some lithic artifacts occurring in DB Sand 4c. However, mean and maximum values are slightly higher than the underlying LB Silts or Laminated Facies, suggesting the excavated areas may be peripheral to the main area of occupation and so not heavily altered or that occupation occurred only once or without a fire being built. DB Sand 4b records the first major enhancement in MS with values up to 17.54. Karkanas and Goldberg (2010) also identify DB Sand 4b as the first

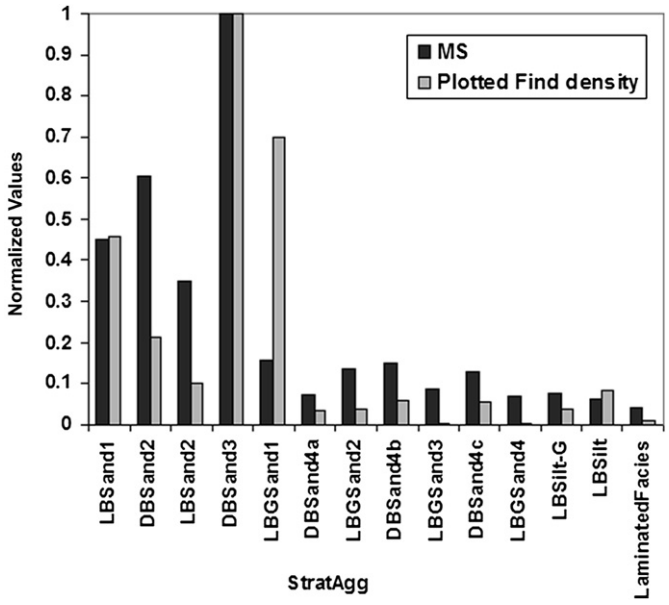

Fig. 11. Comparison between mean MS (10^{-8} m^3 kg^{-1}) values and plotted find density for the various StratAggs from the Western excavations (plotted find density includes archaeological and potentially also non-archaeological material as the plotted finds had not been fully categorized at the time of this analysis).

evidence for anthropogenic alteration in the rear of the cave. DB Sand 4b deposits have age estimates of between 166 and 152 ka, making them statistically contemporary with LC-MSA Lower (174–153 ka). Though due to the lack of shellfish in DB Sand 4b, it is likely that these sediments are slightly younger than the LC-MSA Lower deposits as they were deposited during a short window in time when the sea was at a distance suitable for foraging (Marean et al., 2007). The overlying LBG Sand 2 also records enhanced MS values up to 17.73 and probably dates to around the same period.

DB Sand 4a showed little enhancement when the first deposits from this layer were investigated (max MS 4.28; Table 1). However, recent re-excavation of this area of the cave (not reported in this special issue) suggests that it was extensively utilized by humans during this period, which appears to contrast with the initial MS analysis. Analysis of these new deposits gave MS values of up to 274 associated with a combustion feature, one of the highest values for the site (work in progress). There are a number of potential explanations as to why the initial MS did not identify anthropogenic occupation of DB Sand 4b adjacent to the feature (see above and SOM). Waterlogging is one explanation, but it is more likely that the deposits previously sampled were essentially unaltered due to being peripheral to the main occupation. Figure 12 shows two sections taken vertically through the Western area excavation. One section shows no enhancement until quite near the top of the sequence in DB Sand 3, while the other section shows some limited enhancement from as early as DB Sand 4a. Figure 12 illustrates how simple sections and limited sampling can show very different patterns in the MS signature and hence interpretation of occupation of the site as a whole. It also illustrates that the MS can show how different parts of sites were occupied during different periods.

LBG Sand 1 consists of roof spall, but with an increased input of aeolian beach sand and has an age range of between 134 and 94 ka, probably including two separate occupations split by a hiatus. LBG Sand 1 records greater enhancement with MS values up to 26.32, but the mean MS value is still low (4.74). The MS indicates some alteration or admixing of anthropogenic material, but there is little evidence for major burning. The age estimates for LBG Sand 1 overlap with heavily altered layers in the front of the cave, such as LC-MSA Upper, and suggests preferential use of the front of the cave over the rear at this time.

DB Sand 3 is similar to LBG Sand 1 but darker and sandier and it has an age estimate of between 102 and 91 ka based on OSL ages of deposits above and below it. The brownish color of the unit is linked to an increased anthropogenic input of charcoal and organic matter and also includes burnt bone. Karkanas and Goldberg (2010) state that these layers are strongly influenced by human input. MS from DB Sand 3 are higher than anywhere else in the Western excavation with a mean MS value of 30.0 and a spread in MS between 2.42 and 150.0. The MS analysis indicates that while there are still unaltered areas of the unit, major anthropogenic alteration has occurred in certain areas (Fig. 8). The occurrence of dense ochre deposits and high artifact density from this layer further emphasizes the anthropogenic nature of DB Sand 3 (Figs. 4 and 8). Clusters of high MS (MS hot spots) are, therefore, considered to indicate major areas of *in situ* burning (see SOM video). Burnt material has subsequently been lightly distributed over the area between the hot spots and in particular down slope towards the entrance (east) of the excavation area. DB Sand 3 is likely contemporary with layers from the Eastern excavation (Shelly Brown Sand, Lower and Upper Roof Spall), which all show high MS values (MS up to 414.01) and have been significantly altered by burning. It appears that during DB Sand 3 times, unlike earlier periods, humans were heavily occupying both the front and rear of the cave.

LB Sand 2 has a mean MS value of 13.44, maximum MS values of 22.87, and an age estimate of 102–91 ka. The higher overall values

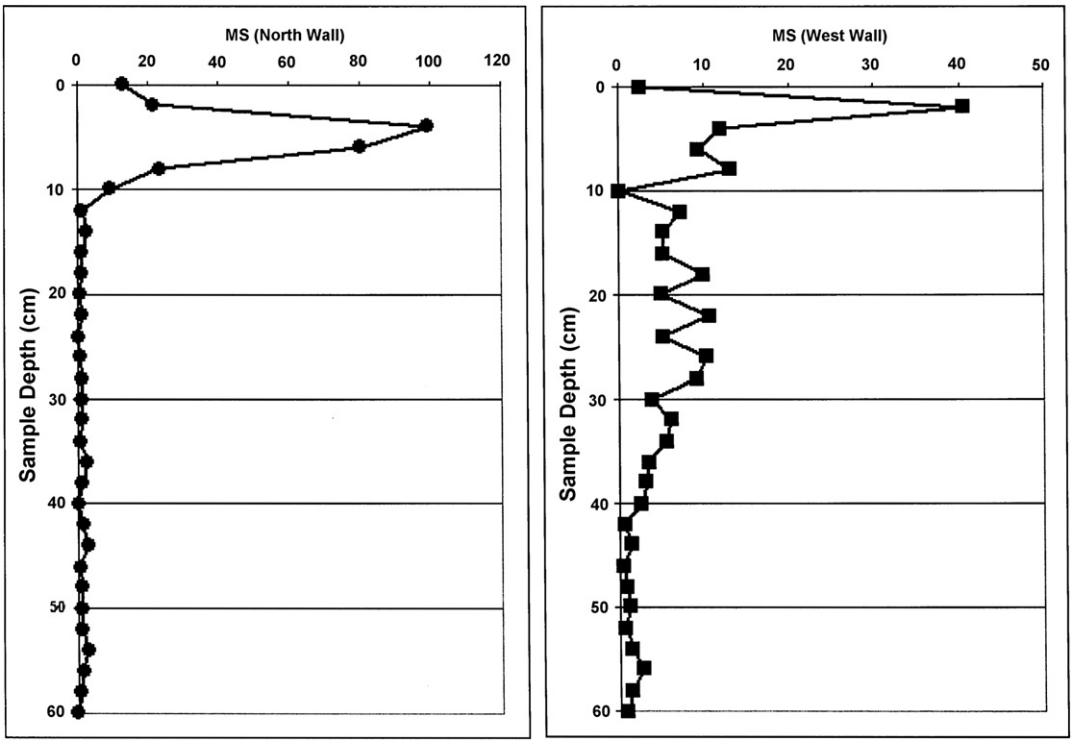

Fig. 12. A comparison of magnetic susceptibility (10^{-8} m^3 kg^{-1}) of two adjacent sections from the north and west wall of the Western (rear) area excavations at PP13B.

of LB Sand 2 suggests that there is significant anthropogenic material, but no evidence of major MS hot spots, which would indicate significant *in situ* combustion features (unless they have been significantly disturbed and intermixed with unburnt sediments). The lack of low MS values, suggesting unaltered sand, indicates some homogenization of the deposits, usually indicating mixing. DB Sand 2 also has an age estimate of 102–91 ka, this is a relatively high mean MS value of 18.16 but its maximum MS value is only 29.92. It has similar properties to LB Sand 2. LB Sand 1 has an age estimate of between 94 and 91 ka and so is slightly younger than or contemporary with DB Sand 2. It represents the last deposit before the cave was sealed. The MS pattern is similar to DB Sand 2 and LB Sand 2.

Overall DB Sand 3 is the only deposit where well-defined MS hot spots occur in the Western area excavation, although a hot spot seems also to occur in the new excavations of DB Sand 4a. The mineral magnetism suggests that there has been minimal enhancement of the Western deposits by anthropogenic action since DB Sand 4c times (349–152 ka), but that it is most noticeable from DB Sand 4b times (166–152 ka). This is not unexpected as there is good evidence for major occupation of the front of the cave (LC-MSA Lower; 174–153 ka) with *in situ* combustion features slightly before this (Marean et al., 2007).

When the vertical distribution of MS data are correlated with plotted find density it is also noted that in many cases stratigraphic aggregates with increased MS have a greater density of plotted finds, and this correlation is particularly noticeable in the Western area excavations (Fig. 10) from LBG Sand 1 (134–94 ka) onwards. Both micromorphology and MS data indicate little evidence for dense anthropogenic alteration of the earlier deposits in the rear of the cave. The overall agreement between plotted find density, micromorphology, and MS values strengthens the argument that MS values, and so anthropogenic alteration, may be a helpful guide in reflecting the intensity of occupation of layers or areas of the cave. When the data are looked at horizontally in the Western excavations (Fig. 9), MS hot spots do not correlate well with artifact density. Density is highest in areas of medium MS values, where mixing of anthropogenic material into unaltered material is suggested. Again the highest density is just down slope of the hot spots towards the front (east) of the excavation area. This is the area that people would have occupied, around the combustion features, and so where activities and hence cultural remains would have accumulated. This is an important pattern in the MS signal and may help to define activity specific areas related to combustion features. In the Eastern area during DB Sand 3 times, people appear to have created fires against the southern and rear wall of the cave and utilized the area towards the cave mouth (east) in the center of the cave.

Correlation with the front of the cave

As noted previously, MS signatures differ significantly between excavation areas (Figs. 3 and 13c and d; Table 1; SOM Fig. 2). The Western area excavation mean MS values are significantly lower than those in the Eastern and Northeastern (LC-MSA) excavation areas and the Western is the only area with a mean value below that for FICF from the site. This reflects the fact that the basal material at the rear of the cave is archaeologically sterile and so the mean for material from the Western area excavation is biased by the number of sterile or low occupation levels. It might seem that this pattern may also reflect the likelihood that fires would have been preferentially built in the front of the cave. However, DB Sand 3 from the rear of the cave has a number of well-defined MS hot spots with MS values up to 150 and thus clear evidence of heavily altered deposits.

The background MS signal in the rear of the cave is lower than for the front of the cave and suggests that the combustion features are relatively undisturbed in DB Sand 3, and so the area had less movement of people disturbing the deposits. The suggested occurrence of *in situ* hearths in DB Sand 3 is somewhat surprising given the fact that they appear to have been built in the interior of the cave and close to the southern wall. Preliminary examination of

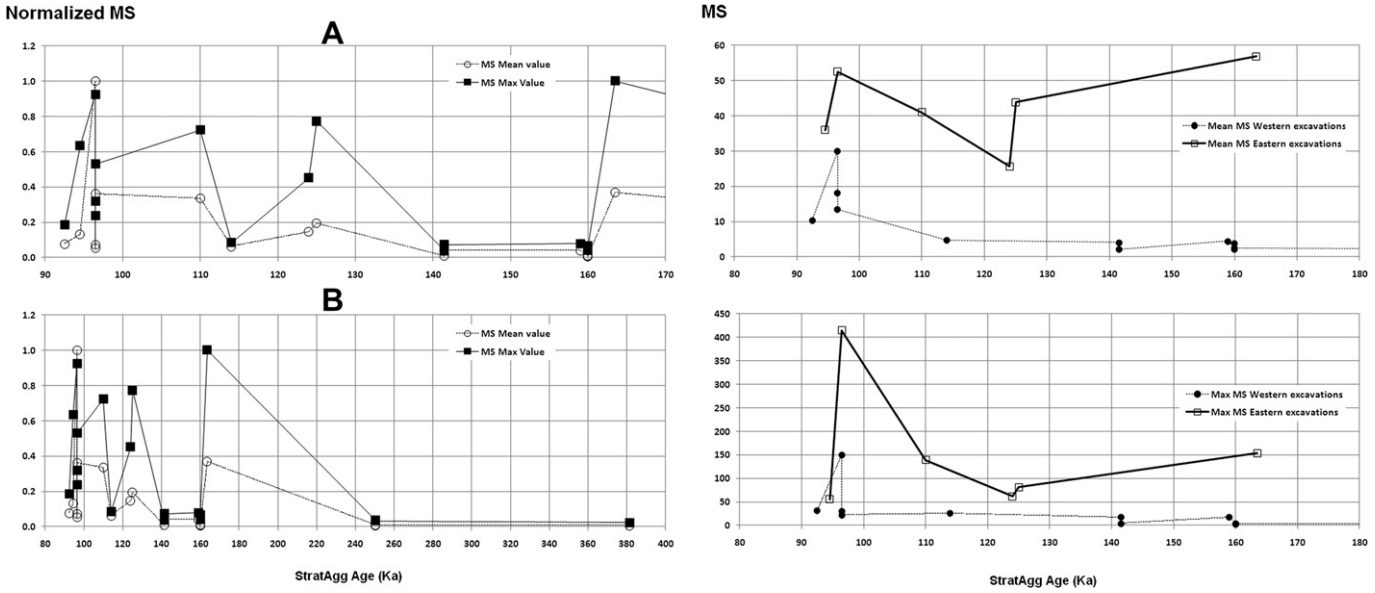

Fig. 13. A comparison of the MS values of StratAggs from different areas of PP13B and through time. (a and b) normalized MS versus maximum (max) and mean MS values through time for the site as a whole, (c) a comparison between the maximum MS values for the Eastern (front) and Western (rear) area excavations through time, (d) a comparison between the mean MS values for the Eastern (front) and Western (rear) area excavations through time.

burnt rocks from PP13B using paleomagnetism suggests that many are not *in situ* (Fig. 1; see Herries [2009] and Brown et al. [2009] for methodology), as the secondary heating remanence within the rock is not oriented in a normal polarity direction (i.e., towards North). These data further support the mixing model suggested by the MS data, but may also point to complex processes such as the raking out and dumping of hearth material.

The MS pattern in the Eastern and Northeastern (front) excavation areas differs from the Western area excavation (Fig. 5), where the MS values appear more homogenous. Maximum values for DB Sand 3, LC-MSA Lower, and Lower Roof Spall from the front of the cave are all around the same MS value ($\sim$150) suggesting perhaps a similar level of occupation. Only one unit has an MS value $<$150; StratUnit E3BD of Upper Roof Spall has an MS value of 414 and represents an undisturbed *in situ*, multiple use combustion feature. Shelly Brown Sand and Upper Roof Spall from the Eastern area excavation appear to contain the remains of a number of combustion features that were likely spread across the entire area, producing a relatively homogenous MS signature horizontally and vertically (Fig. 10). Artifact density for the Eastern area is relatively consistent in its northern half towards the LC-MSA, but much lower in its southern half. However, higher MS values occur in the Southern area. This may reflect a pattern seen in a number of areas in the cave with low artifact density within MSICF and high artifact density in areas adjacent to MSICF. Micromorphology indicates both the presence of *in situ* combustion features and redistributed material that has been trampled in different areas of the section, and confirms the interpretation of the MS pattern (Karkanas and Goldberg, 2010).

The LC-MSA is potentially contemporary with layers in both the Eastern and Western excavation areas. The mean of MS values here (MS = 50.97, $n = 126$) is higher than either of the other two excavation areas within the site (Table 1). The LC-MSA deposits dip $\sim$17° SW and contain clear stratification between unburnt and burnt lenses. The burnt lenses contain ash and dark organic material including carbonaceous material. The spatial distribution of FICF ($n = 22$) here cluster vertically into numerous well-defined lenses. FICF further correlates spatially with the vertical distribution of MS hot spots (MS $>$ 50). The association between FICF and MS hot spots suggests that these deposits contain *in situ* combustion features. Sediment micromorphology analysis of these deposits further supports this conclusion (Karkanas and Goldberg, 2010). Of the three LC-MSA deposits, LC-MSA Lower has the highest MS values (mean 56.76 and max MS 153.49). The LC-MSA deposits contain significant quantities of ochre (utilized and unutilized), shellfish, and lithic material, and artifact density is also high (Fig. 10).

Stratigraphic aggregates from all three excavation areas overlap in time. As such, patterns in the spatial use of the cave can potentially be tracked through time. Figure 13a and b illustrates the difference in MS for the front (Eastern area excavations) and rear (Western area excavation) of the cave through time. The front of the cave has consistently high mean values, except for a slight decline around 124 ka during LC-MSA upper times. This is shortly before or around the period when a large dune occurs in many of the PP caves (Marean et al., 2007, 2010). In contrast, the rear of the cave has consistently low values until less than 102 ka. At this same time a spike in the maximum MS values for the front of the cave is also seen. This pattern seems to indicate a change in the use of space over time, with fire use being concentrated in the front of the cave during earlier periods and then throughout the cave during later periods. The increase in maximum MS in both areas of the cave between 102 and 91 ka may suggest a major occupation phase at this period.

When the MS pattern for all stratigraphic aggregates from different areas of the cave is compared through time (Fig. 13a and b) the pattern of occupation for the cave as a whole can be studied. Low MS values and a lack of occupation by humans dominate until around 164 ka when a spike in MS is noted that correlates with a small rise in sea level, which brings the cave closer to the shoreline (Marean et al., 2007). Humans intensively inhabit the front of the cave collecting shellfish. MS values then return to a low value between 160 and 130 ka, which suggests a lack of intense occupation. This correlates with the end of the cold, glacial MIS 6 period when the cave would have been a long distance from the shoreline. At roughly 130–120 ka high MS values suggest reoccupation of the cave with the advancement of the sea during early MIS 5. A short decline in MS around 120–114 ka seems to suggest

a period of low occupation during a major period of dune formation at the site. After this the entire cave appears to have been intensively occupied until it was sealed by a large dune around 91 ka.

Conclusions

Our answers to those questions posed earlier are: (1) the magnetic mineralogy of the samples supports the use of MS as a proxy of anthropogenically altered material; (2) MS hot spots correlate with StratUnits that were identified as burnt during excavation; (3) micromorphological interpretations correlate well with the MS interpretations; (4) MS data indicate differences between layers from the excavations, but the variation is different for different excavation areas; (5) there is good correlation between MS and plotted find density, which suggests MS is a good proxy for intensity of occupation; moreover, the degree of MS enhancement appears to be a good indicator of occupation longevity and intensity; and (6) there is a major difference in the MS pattern in different excavation areas, which suggests humans were using different parts of the cave more intensively at different time periods.

Deposits from the front of the cave have high MS values during earlier periods when MS is low at the rear of the cave. This indicates a potential change in the occupation pattern of the cave over time. Intense occupation of the front of the cave appears to have occurred during earlier periods with minimal occupation or different activities occurring at the back of the cave during this time. Intense occupation of the entire area of the cave seems to have occurred during later periods, as this is when MS is also high in the rear of the cave. The combustion features seem more intact and less distributed at the rear of the cave when compared to the front, as this is where people would have been entering and leaving the cave. Such changes may reflect fires built for different purposes, such as warmth while sleeping towards the cave rear, and cooking and heat treatment of artifacts towards the front. Changes occurring through time may reflect increasing group sizes utilizing the cave or longevity of occupation at different periods. Distinct spatial patterning can also be noted. A low density of artifacts occurs in areas with high MS, which represent combustion features, while a high density of artifacts occurs in areas of medium MS surrounding the combustion features. These areas adjacent to the combustion features are where the main activities appear to have taken place. Away from these features both artifact density and MS trail off, although some admixture of anthropogenically altered material occurs due to transport from the movement of people.

This first attempt at creating a multidimensional model of MS as a proxy of anthropogenic alteration and distribution for all deposits from an archaeological site has shown a great potential for recovering information about spatial patterning. This type of analysis can also be used to help identify the context of burnt artifacts such as stone tools or ochre. In this way it can be established if such artifacts were associated with combustion features and whether the heating was deliberate. Such an analysis was used by Brown et al. (2009) to help identify the heat treatment of silcrete stone tools from PP5–6. When quantitative analysis of fire-modified rocks and stone tools from a site are combined with MS data as described here, it can provide a very powerful tool for understanding spatial patterning in archaeological sites.

Acknowledgements

Archaeomagnetic analysis was undertaken at the University of Liverpool Geomagnetism Laboratory with the support and assistance of Martin Gratton and Mimi Hill. The work was conducted as part of the Mossel Bay Archaeological (MAP) and SACP4 projects funded by the National Science Foundation (USA; grants # BCS-9912465, BCS-0130713, and BCS-0524087 to Marean), the Hyde Family Foundation, the Institute of Human Origins, and Arizona State University. Additional funding to AIRH was provided by the UNSW Faculty of Medicine and ARC Discovery Grant DP0877603. Thanks to the South African Heritage Resources Agency (SAHRA) and Heritage Western Cape (HWC) for providing permits to conduct excavations at the selected sites and export specimens for analysis. Thanks also to the Mossel Bay community for assisting during excavations and analyses and in particular we thank the staff of the Diaz Museum Complex and the Mossel Bay Archaeological Project.

Appendix. Supplementary data

Supplementary data associated with this article can be found in the online version, doi:10.1016/j.jhevol.2010.07.012

References

Barceló, J.A., 2000. Visualizing what might be. An Introduction to virtual reality in archaeology. In: Barceló, J.A., Forte, M., Sanders, D. (Eds.), Virtual Reality in Archaeology. British Archaeological Reports, vol. S843. ArcheoPress, Oxford, pp. 9–36.

Barceló, J.A., Vincente, O., 2004. Some problems in archaeological excavation 3D modelling. In: Magistrat der Stadt Wien-Referat Kulturelles Erbe-Stadtarchäeologie-Wien (Ed.), Enter the Past. The E-way into the four Dimensions of Cultural Heritage. British Archaeological Reports, Int. Series, vol. 1227. ArchaeoPress, Oxford.

Boukhari, S., 2000. Rebuilding the Past. In: UNESCO Courier, vol. 40.

Brown, K.S., Marean, C.W., Herries, A.I.R., Jacobs, Z., Tribolo, C., Braun, D., Roberts, D.L., Meyer, M.C., Bernatchez, J., 2009. Fire as an engineering tool of early modern humans. Science 325, 859–862.

Church, M.J., Peters, C., Batt, C.M., 2007. Sourcing fire ash on archaeological sites in the Western and Northern Isles of Scotland, using mineral magnetism. Geoarchaeology 22, 747–774.

Dearing, J., 1999. Magnetic susceptibility. In: Walden, J., Oldfield, F., Smith, J. (Eds.), Environmental Magnetism: a Practical Guide. Quatern. Res. Assoc. Tech. Guide, vol. 6, pp. 35–62.

Ellwood, B.B., Petruso, K.M., Harrold, F.B., Schuldenrein, J., 1997. High-resolution paleoclimatic trends for the Holocene identified using magnetic susceptibility data from archaeological excavations in caves. J. Archaeol. Sci. 24, 569–573.

Fisher, E., 2005. Applications of multi-dimensional GIS within subsurface archaeology. Geoconnexion Mag. July/August, 48–50.

Fisher, E., 2007. Beyond smoke and mirrors: applications of multidimensional GIS at two cave/rockshelter sites in Ethiopia and South Africa. In: Paper presented at the 72nd Annual Meeting of the Society for American Archaeology, Austin, Texas, April 26–30, 2006.

Herries, A.I.R., 2006. Archaeomagnetic evidence for climate change at Sibudu Cave. S. Afr. Hum. 18, 131–147.

Herries, A.I.R., 2009. New approaches for integrating palaeomagnetic and mineral magnetic methods to answer archaeological and geological questions on Stone Age sites. In: Fairbrain, A., O'Conner, S., Marwick, B. (Eds.), Terra Australis 28—New Directions in Archaeological Science. The Australian National University Press, Canberra, Australia, pp. 235–253 (Chapter 16).

Herries, A.I.R., Kovacheva, M., Kostadinova, M., Shaw, J., 2007. Archaeo-directional and intensity data from burnt structures at the Thracian site of Halka Bunar (Bulgaria): the effect of magnetic mineralogy, temperature and atmosphere of heating in antiquity. Phys. Earth Planet Int. 162, 199–216.

Herries, A.I.R., Latham, A.G., 2003. 'Environmental archaeomagnetism': evidence for climatic change during the later Stone Age using the magnetic susceptibility of cave sediments from Rose Cottage Cave, South Africa. In: Mitchell, P., Haour, A., Hobart, J. (Eds.), Researching Africa's Past: New contributions from British Archaeologists. Oxford University School of Archaeology Monograph 57, Oxford, UK, pp. 25–35.

Herries, A.I.R., Latham, A.G., 2009. Chapter 5: archaeomagnetic studies at the Cave of Hearths. In: McNabb, J., Sinclair, A.G.M. (Eds.), The Cave of Hearths: Makapan Middle Pleistocene Research Project. University of Southampton Series in Archaeology, vol. 1. Archaeopress, Oxford, pp. 59–64.

Jacobs, Z., 2010. An OSL chronology for the sedimentary deposits from Pinnacle Point Cave 13B - a punctuated presence. J. Hum. Evol. 59 (3-4), 289–305.

Karkanas, P., Goldberg, P., 2010. Site formation processes in site PP13B (Pinnacle Point, South Africa): resolving stratigraphic and depositional complexities with micromorphology. J. Hum. Evol 59 (3-4), 256–273.

Latham, A.G., Herries, A.I.R., 2004. The formation and sedimentary infilling of the cave of hearths and historic cave complex. Geoarchaeology 19, 323–342.

LeBorgne, E., 1955. Susceptibilité magnétiqe anormale du sol superficiel. Annls. Géophys. 11, 399–419.

LeBorgne, E., 1960. Etude expérimentale du trainage magnétique dans le cas d'un ensemble de grains magnétiques trés fins disperses dans une substance non-magnétique. Annls. Géophys. 16, 445–494.
Lewin, J.S., Gross, M.D., 1997. Resolving archaeological site data with 3D computer modelling: the case of Ceren. Automat. Const. 6, 323–334.
Marean, C.W., Bar-Matthews, M., Fisher, E., Goldberg, P., Herries, A.I.R., Karkanas, P., Nilssen, P., Thompson, E., 2010. The stratigraphy of the Middle Stone Age Cave Pinnacle Point 13B (Mossel Bay, Western Cape Province, South Africa). J. Hum. Evol. 59 (3–4), 234–255.
Marean, C.W., Bar-Matthews, M., Bernatchez, J., Fisher, E., Goldberg, P., Herries, A.I.R., Jacobs, Z., Jerardino, A., Karkanas, P., Minichillo, T., Nilssen, P.J., Thompson, E., Watts, I., Williams, H.W., 2007. Early Human use of marine resources and pigment in South Africa during the Middle Pleistocene. Nature 449, 905–908.
Marwick, B., 2005. Element concentrations and magnetic susceptibility of anthrosols: indicators of prehistoric human occupation in the inland Pilbara, Western Australia. J. Archaeol. Sci. 32, 1357–1368.
Mason, R.J., 1988. Cave of Hearths, Makapansgat, Transvaal, Occasional Paper No. 21. Archaeological Research Unit, University of Witwatersrand, Johannesburg, South Africa.
Morinaga, H., Inokuchi, H., Yamashita, H., Ono, A., Inada, T., 1999. Magnetic detection of heated soils at paleolithic sites in Japan. Geoarchaeology 14, 377–399.
Pollefeys, M., Van Goold, L., Vergauwen, M., Conelis, K., Verbiest, F., Tops, J., 2003. 3D recording for archaeological fieldwork. IEEE Computer Graphics Appl., 20–27. May/June 2003.
Peters, C., Batt, C.M., 2002. Dating and sourcing fuel ash residues from Cladh Hallan, South Uist, Scotland, using magnetic techniques. Phys. Chem. Earth Parts A/B/C 27, 1349–1353.
Peters, C., Church, M.J., Coles, G., 2000. Mineral magnetism and archaeology at Galson on the Isle of Lewis, Scotland. Phys. Chem. Earth Part A: Solid Earth Geodesy 25, 455–460.
Peters, C., Thompson, R., 1999. Supermagnetic enhancement, superparamagnetism, and archaeological soils. Geoarchaeology 14, 401–413.
Peters, C., Thompson, R., Harrison, A., Church, M.J., 2002. Low temperature magnetic characterisation of fire ash residues. Phys. Chem. Earth Parts A/B/C 27, 1355–1361.
Redfern, T., Kilfeather, E., 2004. A method for presenting high resolution archaeological 3D scan data in narrative context. In: Proceeding of the 15th International Workshop on Database and Expert Systems Applications (DEXA'04).
Walden, J., Oldfield, F., Smith, J., 1999. Environmental Magnetism: a Practical Guide. In: Quaternary Research Association Technical Guide, vol. 6.
Watts, I., 2010. The pigments from Pinnacle Point Cave 13B, Western Cape, South Africa. J. Hum. Evol. 59 (3-4), 392–411.
Zlatanova, S., Alias, A.A., Rahman, A., Shi, W., 2004. Topological models and frameworks for 3D spatial objects. Comp. Geosci. 30, 419–428.